A&A 404, 505–511 (2003)
DOI: 10.1051/0004-6361:20030558

Astronomy & Astrophysics

Spectropolarimetry of the borderline Seyfert 1 galaxy ESO 323-G077⋆

H. M. Schmid[1], I. Appenzeller[2], and U. Burch[1]

[1] Institut für Astronomie, ETH Zentrum, 8092 Zürich, Switzerland
[2] Landessternwarte Heidelberg-Königstuhl, 69117 Heidelberg, Germany

Received 19 December 2002 / Accepted 31 March 2003

Abstract. We report the detection of high linear polarization in the bright Seyfert 1 galaxy ESO 323-G077. Based on optical spectropolarimetry with FORS1 at the VLT we find a continuum polarization which ranges from 2.2% at 8300 Å to 7.5% at 3600 Å. Similar amounts of linear polarization are found for the broad emission lines, while the narrow lines are not polarized. The position angle of the polarization ($\theta = 84°$) is independent of the wavelength and found to be perpendicular to the orientation of the extended [O III] emission cone of this galaxy. Within the standard model of Seyfert nuclei the observations can be well understood assuming that this AGN is observed at an inclination angle where the nucleus is partially obscured and seen mainly indirectly in the light scattered by dust clouds within or above the torus and the illuminated inner edge of the dust torus itself. Hence we conclude that ESO 323-G077 is a borderline Seyfert 1 galaxy which can provide important information on the geometric properties of active nuclei.

Key words. galaxies: active – galaxies: Seyfert – galaxies: individual: ESO 323-G077 – polarization – scattering

1. Introduction

With $m_V = 13.2$ mag ESO 323-G077 is one of the brightest Seyfert 1 galaxies known. The host galaxy is an SB0 spiral at $z = 0.0150$ with a weak bar and a triaxal bulge (Greusard et al. 2000). The presence of an active nucleus was reported first by Fairall (1986). This relatively late discovery may have been due to the galaxy's location in the less well surveyed southern sky and its relatively low galactic latitude ($b = +22°$). Therefore ESO 323-G077 has not been included in any of the polarimetric surveys of active galaxies like those of e.g. Martin et al. (1983) or Brindle et al. (1990a). No polarimetric observations have been reported in the literature so far. On the other hand, the nuclear colors and the spectrum of ESO 323-G077 indicate substantial reddening (Winkler et al. 1992; Winkler 1992), a property often observed in high-polarization Seyfert 1 galaxies, such as Fairall 51 (Schmid et al. 2001) or Mrk 231 (Smith et al. 1995). This prompted us to obtain for ESO 323-G077 spectropolarimetric observations, which indeed revealed a high linear polarization.

Scattering polarization is well known to occur in Seyfert 2 galaxies and is particularly important for the investigation of aspect-dependent properties of these objects. Spectropolarimetric observations of Seyfert 2s often show the presence of Seyfert 1 type features in polarized light and thus provide the most direct evidence for the standard unified model of AGN (Antonucci & Miller 1985; Antonucci 1993).

As pointed out below the high polarization detected for the ESO 323-G077 appears to be of similar origin as in Seyfert 2 galaxies. However the inclination angle seems to fall in between the typical values for Seyfert 1 and Seyfert 2 galaxies. Therefore, this galaxy offers the opportunity to investigate the geometric properties of the obscuring and light collimating torus assumed in the standard AGN models. Compared to other borderline Seyfert 1 galaxies ESO 323-G077 has the additional advantage that the geometric orientation of the torus can be inferred from the [O III] emission cone which is known to exist in this object from earlier observations.

Following this introduction we outline in Sect. 2 the observations and the data reduction, followed by a description of the spectroscopic and polarimetric properties of the nucleus in ESO 323-G077 in Sect. 3. In Sect. 4 an interpretation of the observations is given.

2. Observations

Optical spectropolarimetry of ESO 323-G077 was obtained during the two nights of January 29 and 31, 2001 with FORS1 (Appenzeller et al. 1998) at the ESO VLT Unit Telescope UT 1 (Antu). Data were taken using the three grisms G300V, G600B and G600R as summarized in Table 1. In all cases a slit width of 1″, a slit height of 20″, and a north-south slit orientation

Send offprint requests to: H. M. Schmid,
e-mail: schmid@astro.phys.ethz.ch

⋆ Based on observations obtained at the ESO VLT UT1 (Antu) at Cerro Paranal, Chile (ESO program 66.B-0063).

Table 1. ESO 323-G077 observing log. t_{exp} is the total exposure time of an entire polarization observation comprising four exposures each.

Grism	Filter	λ-range [Å]	Res. $\lambda/\Delta\lambda$	Date 2001	t_{exp} [min]
ESO 323-G077					
G300V	GG 375	3770–8600	430	Jan. 29	20
G600B		3480–5850	815	Jan. 29	80
G600R	GG 435	5250–7410	1230	Jan. 31	40
GSC 07777-00007*					
G300V	GG 375	3770–8600	430	Jan. 29	4

* star, $m_V = 11.4$ mag, located 30″ west and 6″ north of the ESO 323-G077 nucleus.

was used. The linear polarization was measured using cycles of 4 exposures with different half-wave plate position angles, as described in Schmid et al. (2001). The spectrum was extracted from the central 10″. DIM seeing was always about 1″.

To determine the Galactic interstellar polarization in the direction to ESO 323-G077 we made a short spectropolarimetric observation of the nearby star GSC 07777-00007.

The instrument response curve was determined using wide-slit observations of the spectrophotometric standard star EG 21. This response curve was used to carry out an approximate flux calibration of the relative flux observed through the 1 arcsec slit centered on the nucleus. However, since the observing conditions were not photometric these flux values are of uncertain absolute accuracy, although the relative flux should be correct. Since we found that the calibrated spectra obtained with two different grisms taken on Jan. 29 agree rather well (deviations <5%), we regard the fluxes obtained for that night more reliable. The flux obtained from the G600R spectrum taken on Jan. 31 is 45% lower. Hence we adjusted the flux of the G600R spectrum to the G300V/G600B scale.

Figure 1 combines the spectropolarimetric data of the G600B observation for $\lambda < 5850$ Å and the G600R observation for $\lambda > 5850$ Å. Hα is truncated in order to show the weaker lines and the continuum. The Hα line profile structure is given in Fig. 2a. A flux spectrum without truncation can be found in Fairall (1986). Tables 2 and 3 give flux values and the polarization for emission lines and 250–400 Å wide spectral intervals, respectively.

Due to the longer integration time the signal to noise ratio of the G600B data is higher than for G600R. A small step in the percentage polarization p and the polarized flux $p \times f$ is visible at $\lambda = 5850$ Å. This is probably due to slightly different seeing conditions and slightly different slit positions for the two pointings, resulting in slightly different relative flux contributions from the polarized nucleus and the unpolarized host galaxy. The atmospheric dispersion corrector used with FORS helps to keep such effects small, but they cannot be completely eliminated. In our data, the polarization $p(\lambda)$ of the G600B observation is lower by $\Delta p = 0.13\%$, than for the G300V observation, while p of G600R is 0.14% higher than for G300V. Therefore, whenever possible, mean values were calculated and given in Tables 2 and 3.

The wavelength region from 4050 to 4150 Å in the G600B observation is affected by an optical reflex, which is known to occur for this Grism/Wollaston configuration. The comparison with the reflex-free G300V observation indicates that only the flux spectrum and the relative polarization p are affected, but not the polarized flux and the polarization angle.

In addition we observed spectropolarimetric standard stars (HD 94851, HD 126593, BD+25°727[1]) for estimating the instrument polarization, which was found to be always <0.1% and thus negligible within the accuracy required for this study.

3. Observational results

3.1. The flux spectrum

The observed combined flux and polarization spectra of ESO 323-G077 are displayed in Fig. 1. The flux spectrum shows a flat or slightly reddish continuum (in F_λ) and broad emission lines due to H I, He I and Fe II. Very strong narrow lines are due to [O III] $\lambda\lambda$4959,5007. There are also strong emissions of [O II] λ3726/29, [Ne III] λ3869, [S II] $\lambda\lambda$6716,6731, and there are traces of [N II] λ6583,6548, [O I] λ6300, and [O III] λ4363. On top of the broad H I line components weak, narrow H I lines are clearly visible.

Measured fluxes (uncorrected for slit losses) for the narrow and broad lines and for 250–400 Å-wide flux intervals are given in Tables 2 and 3, respectively. For the H I lines it is difficult to separate accurately the narrow and broad line components. Therefore, we present in Table 2 the flux of the total H I emission. However, the contribution of [N II] to Hα and [O III] to Hγ has been subtracted. About 10% of the total Hα and Hβ line flux are due to the narrow line components. This percentage is uncertain by about a factor of 2 due to uncertainties in the profiles adopted for the broad component, which has been inferred from the comparison of the line profiles in total and polarized flux (Fig. 2, Sect. 3.4).

Our continuum and line fluxes for the stronger lines agree within about 20% with those reported by Winkler (1992).

3.2. Continuum and line polarization

The solid curves in Fig. 1 show the spectroscopic and spectropolarimetric signal obtained for ESO 323-G077. The corresponding polarization parameters, linear polarization p_{obs} and position angles θ_{obs}, are listed in the Tables 2 and 3 for the emission lines and for 250−400 Å spectral intervals, respectively. The parameters p_{obs} and θ_{obs} were calculated from the observed Stokes Q and U spectra according to $p = (Q^2 + U^2)^{1/2}/f$, where f is identical to Stokes I, and $\theta = 0.5 \cdot \arctan(U/Q)$.

The errors of the continuum polarization (Table 3) include the instrumental polarization. The errors of the polarization of the broad lines is strongly affected by the uncertainties in the continuum definition. Therefore, the errors are larger for weaker lines and for the broad Fe II features.

[1] Note that in the list of polarized standard stars of Turnshek et al. (1990) the polarization of BD+25°727 should be $p = 6.27\%$ instead of $p = 4.27\%$ (e.g. Whittet et al. 1992).

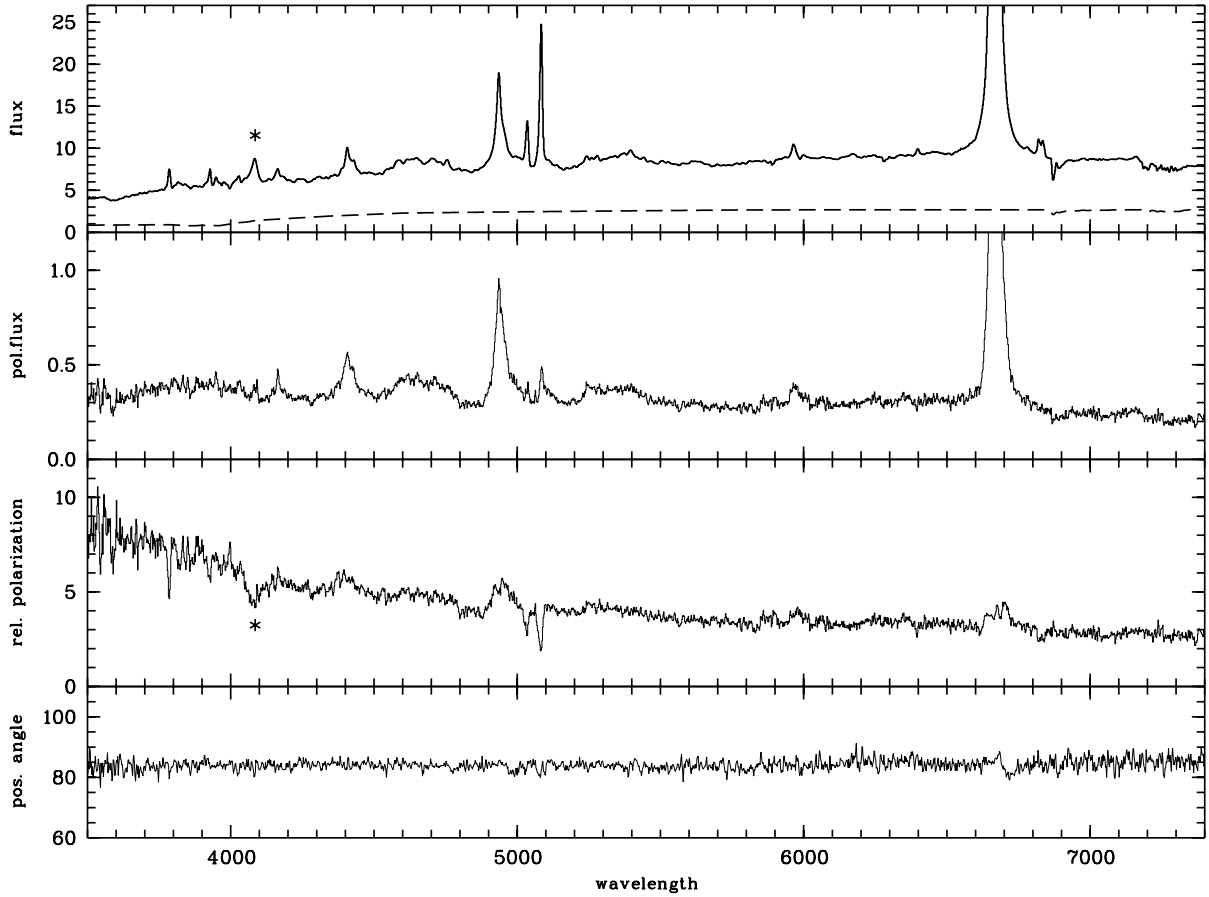

Fig. 1. VLT-spectropolarimetry of ESO 323-G077. The top panel gives the total flux spectrum $f_{\rm obs}$ (in 10^{-15} erg s^{-1} cm^{-2} Å^{-1}) of the bright core (solid line) and the estimated contribution of the host galaxy $f_{\rm gal}$ (dashed line). The polarized flux spectrum $p_{\rm obs} \times f_{\rm obs}$ is plotted in the second panel. The relative linear polarization $p_{\rm obs}$ is displayed in the third panel, and the polarization position angle θ in the bottom panel. The spectral range $\lambda < 5850$ Å is based on the G600B data while the G600R data are plotted for longer wavelength. The asterisks ($*$) at 4050 Å mark an artifact due to the reflex in the G600B spectrum described in Sect. 2.

No significant polarization was measured for the narrow lines. Therefore, the narrow lines are absent in the polarized flux spectrum $p \times f$. The polarization p shows at the position of the narrow lines a sharp minimum due to the dilution of the polarized continuum by the unpolarized narrow-line light.

The observed spectropolarimetric properties of ESO 323-G077 can be summarized as follows:

- The observed linear polarization $p_{\rm obs}$ in the continuum rises from about 2.2% at 8300 Å to 7.8% at 3600 Å. Compared to the total flux, the colours of the polarized flux $p \times f$ are significantly bluer by about $B - V = 0.30$ mag.

- The broad H I lines, but also the Fe II features at λ5200 and λ4750 and He I λ5876, show a higher polarization $p_{\rm obs}$ than the adjacent continuum. The polarization of the Balmer lines decreases from Hδ over Hγ, Hβ to Hα.

- The position angle of polarization is $\theta = 84° (\pm 2°)$, independent of wavelength.

- The narrow [O III] lines and all other forbidden lines show no detectable polarization.

3.3. The possible contribution of the Milky Way ISM to the observed polarization and reddening

Because of the relatively low Galactic latitude $b = +22.4°$ of ESO 323-G077 an interstellar reddening and a possible Galactic interstellar contribution to the observed polarization has to be considered. According to the far-IR dust emission (Schlegel et al. 1998 / NED database) an interstellar reddening of $E_{B-V} = 0.10$ is to be expected in the direction of ESO 323-G077.

Some information on the interstellar polarization in this direction is provided by our observations of the star GSC 07777-00007 located only 30″ from the nucleus of ESO 323-G077. For this star we find a continuum polarization of $p = 0.22\%$, $\theta = 177°$. A literature search yields similar values for the interstellar reddening and polarization of other distant stars in the general region of ESO 323-G077, e.g. for the the two B stars HD 112192 and HD 114981 (Mathewson & Ford 1970; Hill 1970; Kilkenny et al. 1975). Hence we conclude that the result for GSC 07777-00007 can be regarded as representative for this direction.

Our observed spectrum indicates that GSC 07777-00007 is a late F star, or an early metal deficient G star. It seems safe

Table 2. Observed emission line properties. The flux $f_{\rm obs}$ is given in 10^{-15} erg s^{-1} cm^{-2}. Upper $p_{\rm obs}$-limits are given for stronger lines without a significant polarization detection. Note that the fluxes refer to a 1 arcsec slit with seeing losses.

$\lambda_{\rm obs}$ [Å]	Line	$f_{\rm obs}$ [10^{-15}]	$p_{\rm obs}$ [%]	$\theta_{\rm obs}$ [°]	Errors [%/°]
3785.5	[O II]	22	<3		
3927.3	[Ne III]	16	<2		
3948.9	H8	8			
4027.5	[Ne III]	6			
4163.4	Hδ	21	11.6	75.1	5.8/13.3
4407.6	Hγ	79	9.8	81.4	1.9/5.5
4427.9	[O III]	4			
	Fe II	298	6.7	81.7	1.0/4.2
4926.1	Hβ	389	6.4	83.2	0.5/2.2
5034.5	[O III]	60	<2.5		
5083.5	[O III]	213	<1.0		
	Fe II	265	5.6	84.8	1.1/5.6
5965.5	He I	30[a]		78.9	/8.1
6398.6	[O I]	8			
6663.3	Hα	2410	3.9	84.7	0.1/0.7
6683.0	[N II]	90			
6820.2	[S II]	20	<1.5		
6834.4	[S II]	23	<1.5		

Table 3. Measured mean flux $f_{\rm obs}$ (in 10^{-15} erg s^{-1} cm^{-2} Å^{-1}) and polarization $p_{\rm obs}$, $\theta_{\rm obs}$ of ESO 323-G077 for selected intervals in the observed wavelength frame. The flux and polarization of the active nucleus $f_{\rm agn}$, $p_{\rm agn}$ are derived after correction for the estimated dilution by the host galaxy and narrow lines. Note that the fluxes refer to a 1 arcsec slit with seeing losses.

Interval $\lambda\lambda_{\rm obs}$	$f_{\rm obs}$	$p_{\rm obs}$ [%]	$\theta_{\rm obs}$ [°]	$f_{\rm agn}$	$p_{\rm agn}$ [%]
3500–3750	4.2	7.77	83.5	3.3	9.89
3750–4000	5.3	6.70	84.1	4.3	8.26
4000–4250	6.0	5.85	84.7	4.6	7.63
4250–4500	6.9	5.35	84.5	5.0	7.38
4500–4850[a]	7.7	4.70	84.0	5.4	6.70
4850–5150[b]	9.7	4.15	83.9	6.5	6.19
5200–5600	8.4	3.94	84.1	5.9	5.60
5600–6000	8.3	3.51	84.2	5.7	5.11
6000–6400	8.7	3.30	84.7	6.0	4.79
6400–6800[c]	15.5	3.49	84.4	12.8	4.23
6800–7200	8.8	2.74	85.0	6.1	3.95
7200–7600[d]	8.9	2.63	85.2	6.3	3.71
7600–8000[d]	8.6	2.46	85.1	6.1	3.47
8000–8400[d]	8.5	2.25	85.7	6.0	3.19

[a] Includes the strong Fe II λ4550 emission.
[b] Includes the strong Hβ and [O III] emission lines.
[c] Includes the strong Hα line.
[d] Includes strong telluric absorption, which are not corrected for the $f_{\rm obs}$ and $f_{\rm agn}$ values.

to assume that such a star is intrinsically unpolarized. The observed spectrum and the apparent magnitude ($m_V = 11.4$ mag) yields a minimum distance $d > 300$ pc and a minimum distance to the galactic symmetry plane of about 150 pc. Hence the light path to this star passes through most of the galactic dust layer. The observed polarization of this star can, therefore, be regarded as characteristic for the Galactic interstellar polarization of extragalactic objects in this direction. If this is the case, the Galactic interstellar polarization along the line of sight is very small compared to the intrinsic polarization of ESO 323-G077. Moreover, the position angle of the interstellar polarization $\theta = 177°$ is practically perpendicular to the intrinsic polarization $\theta = 84°$. Hence, an interstellar polarization correction would enhance the intrinsic polarization by about 0.2% without changing the angle significantly. Since systematic errors in the derivation of the relative contribution of the unpolarized light of the host galaxy to the polarized nuclear spectrum introduce larger uncertainties, and since there may be local variations of the Galactic interstellar polarization no attempt was made to correct for the small Galactic polarization.

3.4. Polarization structure of the emission lines

Figure 2 shows the line profiles for the total flux f and for the polarized flux $p \times f$ of the strongest emission lines. In each case the continuum flux has been subtracted. In the case of Hα weak narrow nebular [N II] lines are superimposed. Apart from small effects resulting from this blending, the line profiles of the broad components of Hα and Hβ are obviously very similar in the total and in the polarized flux. On the other hand, the narrow nebular lines [O III] near Hβ and [N II] at 6683 Å are very weak or absent in the polarized light. The same seems to be true for the narrow line components of Hα and Hβ. Thus, the line profile in polarized flux can be used as guide for separating the broad line components from the narrow line components in the total flux spectrum. We used this to estimate the relative contribution of the narrow component to the total line flux for Hα and Hβ (see Sect. 3.1).

Figure 2 also indicates that the polarization in the blue wing and the line center of the broad Hα component is about $p = 4.5\%$, while it is higher than 5% in the red wing around 7000 Å. For the broad Hβ component the blue wing and line center have a polarization of about 7%, while the red line wing shows about 8%. The polarization of the entire Hα and Hβ features as given in Table 2 are lower because of the contribution of the unpolarized narrow line components.

Moreover we see for Hα in the position angle spectrum in Fig. 1 a small position angle rotation of about 8° from the blue line wing to the red line wing. Such structures in the polarization angle are often seen in high quality data of the Hα-lines in Seyfert 1 galaxies (e.g. Goodrich & Miller 1994; Young et al. 1999; Schmid et al. 2000; Smith et al. 2002). It is beyond the scope of this paper to investigate the nature of this effect. The interested reader is refered to the detailed description and discussion in Smith et al. (2002).

4. Interpretation

Seyfert 1 galaxies with high scattering polarization are rare (e.g. Smith et al. 2002). Good examples are Mrk 231, Mrk 486, Mrk 704 and Fairall 51 (Goodrich & Miller 1994;

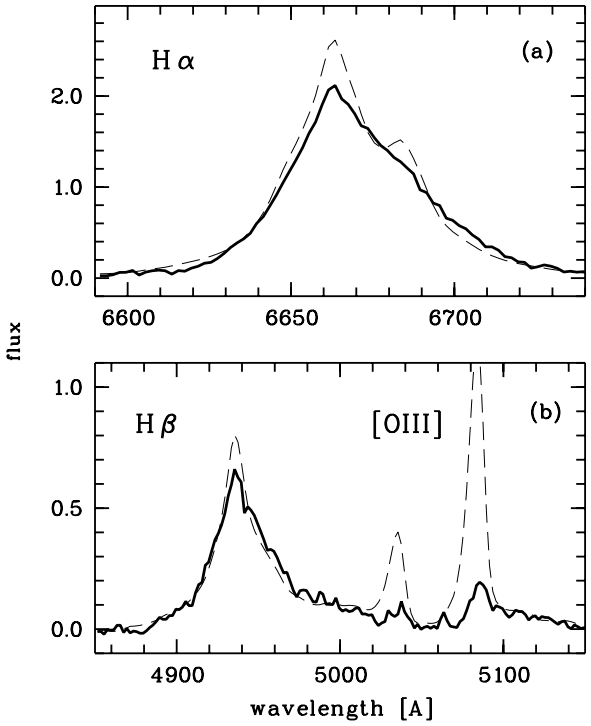

Fig. 2. Line profiles of the **a)** Hα and **b)** Hβ and [O III] emission lines for polarized light $p \times f$ (solid line) and total light f (dashed line). The flux scales (in 10^{-15} erg s^{-1} cm^{-2} Å^{-1}) refer to the $p \times f$ spectra. The f-spectra are scaled by factors of 0.045 for Hα and 0.07 for Hβ/[O III] for this comparison of the broad line structure in f and $p \times f$.

Smith et al. 1995, 1997; Schmid et al. 2001). ESO 323-G077 is a new member of this group. In the following discussion we adopt for ESO 323-G077 the analysis procedure developed and described by Schmid et al. (2001) for the high-polarization Seyfert 1 galaxy Fairall 51. This appears reasonable since both objects have very similar spectropolarimetric properties.

Important for the spectropolarimetric analysis of Seyfert nuclei is an estimate of the host galaxy's contribution to the intensity spectrum. In contrast to F51 our spectra of ESO 323-G077 show no undisturbed spectral features from the host galaxy which could be used to estimate the host galaxy's contribution. Therefore, we rely on the assumption that the broad lines and continuum from the nucleus have at a given wavelength the same polarization, i.e. the relative polarization spectrum $p_{\rm AGN} = p_{\rm obs} \times f_{\rm obs}/f_{\rm AGN}$ is essentially featureless apart from a slope from blue to red. This is expected if the nuclear spectrum and the broad lines have the same scattering geometry, which is to be expected if the scattering occurs far away from the nuclear continuum and broad line emission region. On the basis of this assumption we subtracted from the observed spectrum a scaled "typical" galaxy spectrum, with the scaling factor adjusted to reach a polarization in the broad lines equal to the adjacent continuum. As a "typical" galaxy spectrum we used that of the E0 galaxy NGC 3379 (Kennicutt 1992), which should be a reasonable approximation for the central (bulge) region of the ESO 323-G077 host galaxy. The relative flux of the host galaxy spectrum $f_{\rm gal}$ derived in this way has been plotted in the top panel of Fig. 1 as a dashed line. Table 3 gives the resulting flux $f_{\rm AGN} = f_{\rm obs} - f_{\rm gal} - f_{\rm NLR}$ and polarization $p_{\rm AGN}$ for the active nucleus. For this purpose we also subtracted the narrow line emission $f_{\rm NLR}$.

According to the study on Fairall 51, the nuclear spectrum $f_{\rm AGN}$ can be further separated into direct $f_{\rm d}$ and scattered $f_{\rm s}$ light. These components must have the following properties in order to explain the presence of a high scattering polarization (see Schmid et al. 2001):

- $f_{\rm d}$ must pass through a dust layer producing an attenuation and reddening of the direct (unpolarized) light;
- a sufficiently large scattering region must be present and visible from us which can produce the observed fraction of polarized nuclear light;
- the scattering angle has to be of the order ≈45° to produce a sufficiently high polarization.

The spectrum of ESO 323-G077 obviously shows all spectral components required by the model. The amount of the observed polarization is slightly lower but of the same order as in the case of Fairall 51. Hence, the relative contributions to the observed light are similar. Thus, the new observations strongly support the general scenario outlined for the case of Fairall 51 and illustrated by Fig. 6 of Schmid et al.(2001). In this model the circumnuclear torus is inclined so that the direct light from the central source has a line of sight close to the torus walls where substantial reddening occurs. The high polarization is due to scattering by optically thin dust located in polar directions above and inside the torus. The scattering angle and therefore the inclination of the torus plane must be around ≈45° with respect to the line of sight in order to explain the high scattering polarization in ESO 323-G077 and Fairall 51. For smaller inclinations the scattering angle would be too small to produce a strong polarization signal (as in normal Seyfert 1s), while for larger inclinations the direct (unpolarized) emission from the continuum source and the BLR would be completely hidden by the torus as in Seyfert 2s.

While the data described here support the qualitative model developed on the basis of Fairall 51, the new data of ESO 323-G077 contain important additional information concerning the scattering geometry. Important is that the polarization position angle (PA) defines the relative orientation of the scattering region with respect to the light source, since the $\boldsymbol{E}$ vector of the scattered light has to be perpendicular to the scattering plane (the plane containing the incident and scattered ray). As shown by Fig. 3 the observed PA of polarization in ESO 323-G077 is within the limits of the observational errors perpendicular to the PA of the extended [O III] emission region observed by Mulchaey et al. (1996a) for this galaxy. This is exactly the orientation which we have to expect if the observed extended [O III] emission originates in an ionization cone produced by the non-isotropic radiation field of the AGN.

Such [O III] emission regions are seen in many Seyfert 2 galaxies (e.g. Pogge 1989; Mulchaey et al. 1996a,b) and are normally taken as evidence for an emission of the ionizing radiation from the active nucleus along the symmetry axis of the disk and torus system present according to the unified model of Seyfert galaxies (Antonucci & Miller 1985; Krolik & Begelman 1988; Antonucci 1993). Apart from

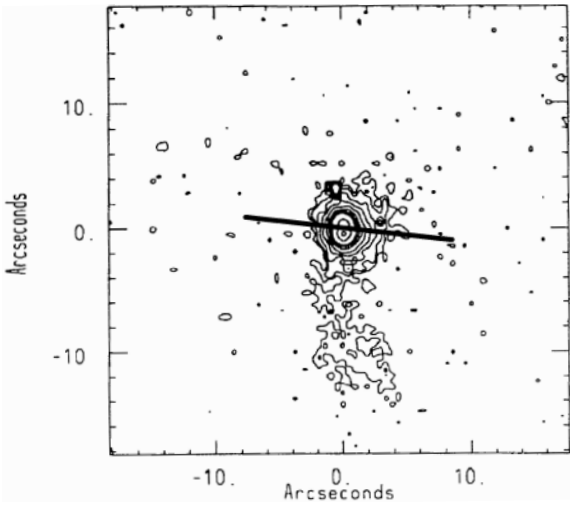

Fig. 3. Comparison of the orientation of the of the extended [O III] emission in ESO 323-G077 (map from Mulchaey et al. 1996a) and of the orientation of the observed scattering polarization.

Seyfert 2 galaxies the perpendicular alignment between the polarization and the objects symmetry axis has also been observed in narrow-line radio galaxies (the AGN type 2 equivalent to the type 1 broad-line radio galaxies, see e.g. Cohen et al. 1999).

In Seyfert 1 galaxies the situation is more complicated. For those low polarization Seyfert 1s where radio structures or extended emission line regions have been detected the position angle of polarization can be parallel or perpendicular to these structures (Smith et al. 2002).

What is the situation for Seyfert 1s with high scattering polarization? In Mrk 231 the polarization is clearly perpendicular to a well defined radio structure (Goodrich & Miller 1994; Neff & Ulvestad 1988). With ESO 323-G077 we have now another case of a high polarization Seyfert 1 galaxy which shows a perpendicular alignment between polarization and extended nebular emission. We are not aware that extended radio structures or emission line regions have been detected in other systems of this class. Thus, the high polarization Seyfert 1 galaxies ESO 323-G077 and Mrk 231 behave like Seyfert 2 galaxies. Therefore, they strongly support the dust torus induced ionization cone model within the unification scheme which suggest that Seyfert 1 and 2 nuclei are the same physical objects viewed at different orientations.

Hence, the new data and in particular the orientation of the polarisation with respect to the observed [O III] emission strongly support our assumptions that the high-polarization Seyfert 1 galaxies, like ESO 323-G077, Fairall 51, Mrk 231 and probably others, are AGN with orientations very close to the transition between Seyfert 1 and Seyfert 2. In these borderline Seyfert 1 objects a major fraction of the observed light from the nucleus is scattered light reaching us via illuminated dust regions. These could be optically thin dust clouds within or above the torus and/or the illuminated inner edge of the dust torus itself. The other part of the light reaches us directly but significantly reddened by dust extinction in the semi-transparent inner boundary region of the torus.

5. Conclusions

We have shown that the high polarization of the Seyfert 1 galaxy ESO 323-G077 has very similar properties as observed earlier in Fairall 51. As for Fairall 51, the observations of ESO 323-G077 can be understood assuming that the AGN is observed at an inclination of roughly $\approx 45^\circ$, so that the nucleus is partially obscured by the torus and where scatterings by dust in polar directions above or within the torus produce the high linear polarization.

The fact that in the case of ESO 323-G077 the observed polarization is found to be perpendicular to the AGN's projected symmetry axis, as deduced from the orientation of the extended [O III] emission region, supports the dust torus induced ionization cone model.

The finding that the inclination angle of the active nuclei in ESO 323-G077 and Fairall 51 cannot be much different from 45 degrees, provides important constraints on the aspect ratio of the AGN dust tori. Further information on this question could be derived from the frequency of objects like ESO 323-G077, Fairall 51, and Mrk 231, which must be regarded in the unified model for Seyfert galaxies as borderline cases between type 1 and type 2 systems. Because of the constraints on the inclination angles which can be derived from the amount of observed polarization, these high polarization Seyfert 1 galaxies can play an important role for determining the geometric properties of AGN. Therefore, it will be very desirable to look for further examples of this apparently rare class of Seyferts in order to obtain a meaningful sample for a statistical evaluation of their properties.

Acknowledgements. We thank the referee, A. Robinson, for thoughtful comments and for pointing out the observations of the radio structure in Mrk 231 in the literature.

References

Antonucci, R., & Miller, J. 1985, ApJ, 297, 621
Antonucci, R. 1993, ARA&A, 31, 473
Appenzeller, I., Fricke, K., Fürtig, W., et al. 1998, ESO-Messenger, 94, 1
Brindle, C., Hough, J. H., Bailey, J. A., et al. 1990a, MNRAS, 244, 577
Brindle, C., Hough, J. H., Bailey, J. A., et al. 1990b, MNRAS, 244, 604
Cohen, M. H., Ogle, P. M., Tran, H. D., Goodrich, R. W., & Miller, J. S. 1999, AJ, 118, 1963
Fairall, A. P. 1986, MNRAS, 218, 453
Goodrich, R. W., & Miller, J. S. 1994, ApJ, 434, 82
Greusard, D., Friedly, D., Wozniak, H., Martinet, L., & Martin, P. 2000, A&AS, 145, 425
Hill, P. W. 1970, MNRAS, 150, 23
Kennicutt, R. C. 1992, ApJS, 79, 255
Kilkenny, D., Hill, P. W., & Schmidt-Kaler, Th. 1975, MNRAS, 171, 353
Krolik, J. H., & Begelman, M. C. 1988, ApJ, 329, 702
Martin, P. G., Thompson, I. B., Maza, J., & Angel, J. R. P. 1983, ApJ, 266, 470

Mathewson, D. S., & Ford, V. L. 1970, Mem. R. Astron. Soc., 74, 139
Mulchaey, J. S., Wilson, A. S., & Tsvetanov, Z. 1996, ApJS, 102, 309
Mulchaey, J. S., Wilson, A. S., & Tsvetanov, Z. 1996, ApJ, 467, 197
Neff, S. G., & Ulvestad, J. S. 1988, AJ, 967, 841
Pogge, R. W. 1989, ApJ, 345, 730
Schlegel, D. J., Finkbeiner, D. P., & Davis, M. 1998, ApJ, 500, 525
Schmid, H. M., Appenzeller, I., Camenzind, M., et al. 2000, Proc. SPIE, 4005, 264
Schmid, H. M., Appenzeller, I., Camenzind, M., et al. 2001, A&A, 372, 59
Smith, P. S., Schmidt, G. D., Allen, R. G., & Angel, J. R. P. 1995, ApJ, 444, 14
Smith, P. S., Schmidt, G. D., Allen, R. G., & Hines, D. C. 1997, ApJ, 488, 202
Smith, J. E., Young, S., & Robinson, A., et al. 2002, MNRAS, 335, 773
Turnshek, D. A., Bohlin, R. C., Williamson, R. L., et al. 1990, AJ, 99, 1243
Whittet, D. C. B., Martin, P. G., Hough, J. H., et al. 1992, ApJ, 386, 562
Winkler, H., Glass, I. S., van Wyk, F., et al. 1992, MNRAS, 257, 659
Winkler, H. 1992, MNRAS, 257, 677
Young, S., Corbett, E. A., Giannuzzo, M. E., et al. 1999, MNRAS, 303, 227